Nucleation and Void Formation Mechanisms in SiC Thin Film Growth on Si by Carbonization

J. P. Li* and A. J. Steckl**

Nanoelectronics Laboratory, Department of Electrical and Computer Engineering, University of Cincinnati, Cincinnati, Ohio 45221-0030

ABSTRACT

The nucleation mechanisms for SiC thin films on Si were investigated by interrupting the growth at very brief times (~1 to 10 s) using rapid thermal chemical vapor deposition in conjunction with hydrocarbon carbonization. The resulting SiC nuclei and films on Si have been studied by scanning electron microscopy and atomic force microscopy. The hydrocarbon partial pressure in the gas stream was found to determine the nucleation mode. Low precursor concentration results in initial three-dimensional (island) growth which enables the study of trench and void formation. Voids were observed to initiate when two neighboring nuclei come in contact. Trenches in the Si substrate surround each isolated nucleus, with the trench depth increasing with the diameter of the island. SiC films grown for a nominal reaction time of 1 s indicate that increasing the propane concentration results in decreases in SiC grain size and surface roughness and an increase in the nuclei density. A model is proposed for the nucleation process of SiC growth on Si by carbonization consisting of the following key steps: (*i*) the initial nucleation density is determined by the precursor concentration; (*ii*) lateral and vertical growth of individual nuclei proceeds by consumption of Si atoms around their periphery, forming trenches in the substrate; (*iii*) Si voids are formed in the Si substrate near the SiC/Si interface when nuclei grow large enough to come in contact and, thus, restrict the supply of Si atoms.

Introduction

The growth of SiC thin films on Si is one of the most difficult challenges of heteroepitaxy due to the large mismatches in lattice constant (20%) and thermal expansion coefficient (~8%) between cubic (3C) SiC and Si. Relatively thin SiC layers can be formed on Si by carbonization, in which the Si surface is exposed to a C containing precursor at high temperature and is converted into SiC. This process is intrinsically selective on Si with an SiO_2 mask and enables a relatively simple and direct incorporation of SiC into the mature Si processing technology.

Early SiC films formed by carbonization were found to be polycrystalline by some authors[1] and crystalline by others[2-4] when grown beyond a certain thickness.[5] It was found that thicker films can be formed at lower temperatures using very low pressure growth.

Thicker SiC films can be obtained on the converted layer by chemical vapor deposition (CVD) growth with both C and Si containing precursors in the gas stream. This process has been employed by many researchers[6-11] to grow SiC films. The carbonized layer, also known as a buffer layer, is relatively thin (<1000 Å) and plays an important role[6,8,9,12] in the subsequent bulk growth. Temperature ramp-up during carbonization was found necessary for single-crystal growth.[8,9] Initially the buffer layer was thought to be a transition layer, however, detailed high-resolution transmission electron microscope (HRTEM) studies[13-17] later indicated that even Si and C atoms at the SiC/Si interface take the bulk SiC arrangement.

Even though monocrystalline SiC films have been obtained by this two-step CVD technique, the SiC/Si interface has been plagued with the concurrent formation of voids in the Si substrate.[8,9] The voids are usually hollow inverted pyramids lying just beneath the film. This poses a severe problem in device applications of SiC films on Si. For example, one of the most promising applications of SiC, the wide bandgap emitter SiC/Si heterojunction bipolar transistor (HBT), requires an excellent interface. It has been shown[18-20] by the present authors that void-free SiC films could be formed under certain growth conditions, with the propane partial pressure being the determining factor. This observation relates strongly to SiC nucleation on Si. It is the main objective of this paper to discuss the nucleation mechanisms based on observations regarding SiC growth on Si from our experiments and from the literature.

The SiC films employed in this study were grown by rapid thermal CVD (RTCVD). The RTCVD technique uses continuous gas flow of appropriate precursors in conjunction with the rapid heating and cooling capability of low thermal mass rapid thermal processing equipment to control the growth process. Growth takes place only during the limited period the system is at high temperature. A heating-up rate as fast as 250°C/s is achievable in the system used in this work. Due to fast temperature switching and the precise control over the temperature profile, RTCVD

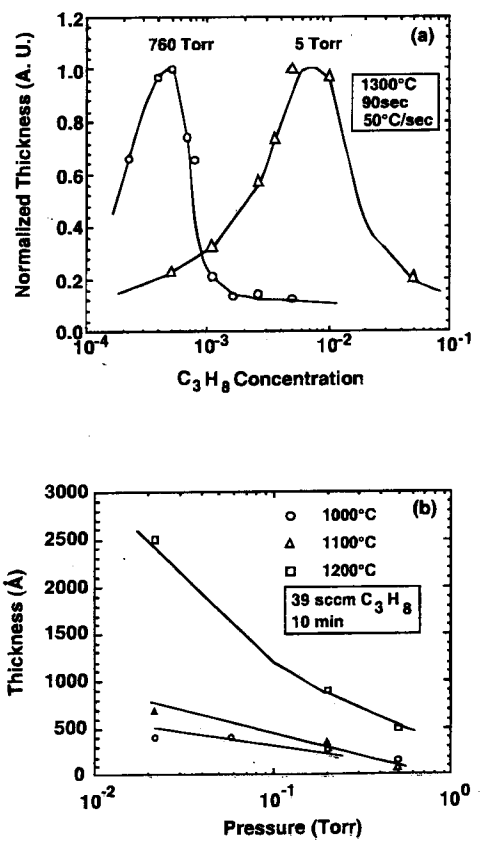

Fig. 1. SiC film thickness *vs.* (a) C_3H_8 concentration at 5 and 760 Torr; (b) growth reaction pressure in the milliTorr range with a fixed flow of 39 sccm C_3H_8.

* Electrochemical Society Student Member.
** Electrochemical Society Active Member.

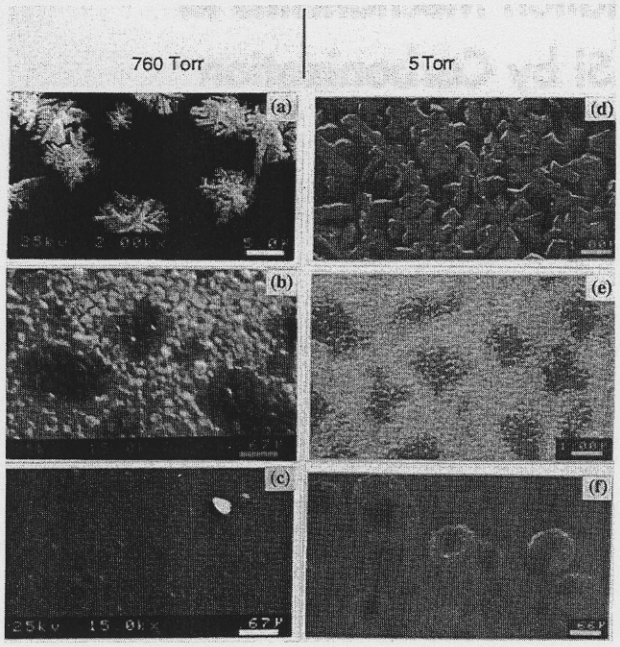

Fig. 2. Surface morphology of films grown at 760 and 5 Torr with different propane flow rate: (a) 4, (b) 7, (c) 30 sccm and additional 0.9 lpm H_2; (d) 10 sccm and 0.9 lpm H_2, (e) 100 sccm and 0.9 lpm H_2, (f) 100 sccm.

can effectively "freeze" the growth at the desired temperature and reaction time. Therefore, RTCVD provides an ideal technique for creating SiC films at various stages of nucleation on Si.

Atomic force microscopy (AFM) was employed for characterizing the carbonized Si surface obtained under various growth conditions. AFM is a powerful, yet relatively easy to use, technique for surface topography analysis.[21-23] Surface analysis with nanometer-scale vertical and horizontal resolution can easily be obtained by AFM. Along with the RTCVD growth technique, this makes AFM an ideal tool for accomplishing the main objectives of this study, namely, the understanding of initial nuclei formation during SiC growth on Si, SiC nuclei growth, and coalescence into a thin film, and concomitant formation of voids in the Si along the SiC/Si interface.

Experimental Procedures

Detailed information on the growth technique and the RTCVD system can be found in Ref. 18. Si (100) wafers were used as substrates for all SiC growth experiments reported here. The SiC films studied here were formed by a two-step process after loading in the growth chamber: *in situ* HCl/H_2 cleaning and carbonization. *In situ* cleaning was carried out at atmospheric pressure at a temperature of 1200°C for 2 min. Typical carbonization conditions were: reaction time of 90 s, temperature ramp rate of 50°C/s, 0.9 slpm H_2 carrier gas, growth temperatures from 1100 to 1300°C. C_3H_8 and CH_4 (both diluted to 5% in H_2) with flow rates from 4 to 100 sccm were used at both atmospheric and low (5 Torr) pressures. These conditions give rise to SiC films with thicknesses from about 100 to 2500 Å. The thickness was measured by cross-sectional scanning electron microscopy (SEM). Relative thickness measured by ellipsometry was used as a reference.

A Digital Instruments (DI) Nanoscope II STM/AFM system was used to study the surface topography of the grown SiC films. A long AFM scan head, with 70 × 70 μm scan area, was used to study large 3-D SiC islands formed at low hydrocarbon partial pressures. A short AFM scan head (0.4 × 0.4 μm scan area) was used to study the initial SiC nucleation after a very short reaction time.

Experimental Results

We have previously reported[18,19] that SiC films grown on Si by carbonization are strongly affected by the precursor concentration in the gas stream in two major aspects: thickness and void formation. The film thickness *vs.* propane concentration for a fixed reaction time indicates that there exists a transition concentration for maximum film thickness, as shown in Fig. 1a. Contrary to conventional CVD behavior, films grown at higher propane concentration are much thinner than those grown at or near the transition concentration. In the case of even lower pressure growth (in the milliTorr range), the film thickness decreases with increasing growth pressure with a fixed C_3H_8 flow rate, as shown in Fig. 1b. This behavior can be seen to be essentially the same as that seen in Fig. 1a where we use C_3H_8 partial pressure as the variable parameter, since the latter is the product of C_3H_8 concentration in the gas and the system pressure. Concurrently formed with thicker films at around the transition concentration are hollow spaces underneath the film in the Si substrate. These empty spaces, also known as voids, take the shape of inverted pyramids with faces parallel to the <111> crystallographic planes.

As shown in Fig. 2, the surface morphology of films grown with increasing hydrocarbon concentrations un-

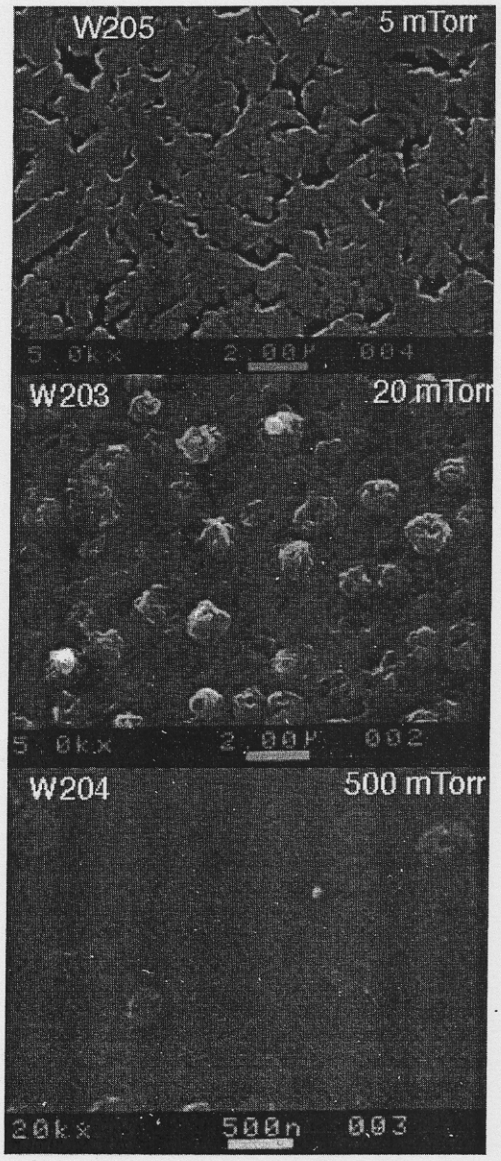

Fig. 3. Film morphology *vs.* growth pressure in the milliTorr range with 39 sccm C_3H_8 flow.

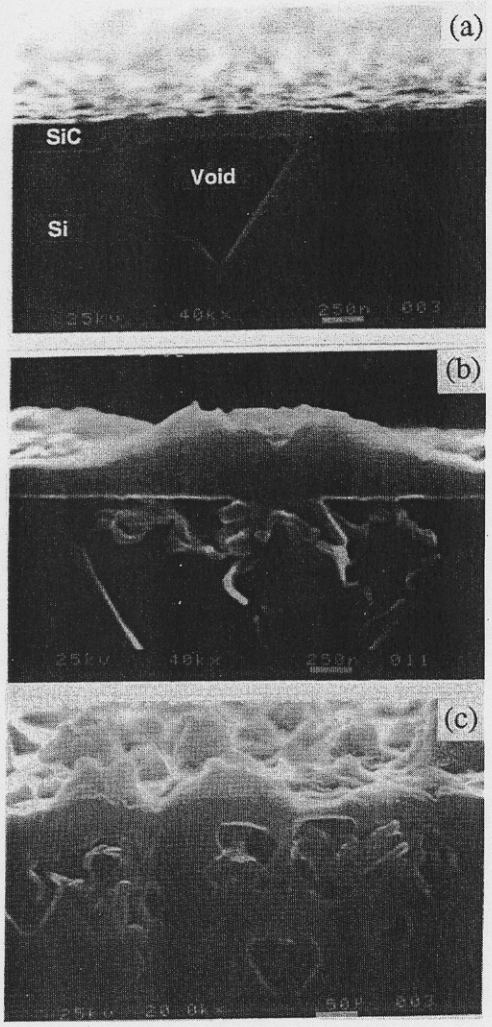

Fig. 4. Voids revealed under cross-sectional SEM for films grown at: (a) 760, (b) 5 Torr, and (c) 22 mTorr.

dergo a change from dendritic island-like features, to continuous films with voids, to ultrathin films. This is true for growth at both atmospheric (AP) and low pressures (LP). However, in the case of LP growth at 5 Torr, additional hillock-like features appear on the film surface at high hydrocarbon concentration. The voids, usually with a rectangular or square cross section along the basal plane, appear dark under SEM observation. The average void size decreases, while the void density increases with increasing hydrocarbon concentrations under otherwise same growth conditions.

The surface morphology of films grown in the milliTorr range with a C_3H_8 flow rate of 39 sccm undergoes a similar transformation with growth pressure, as shown in Fig. 3. However, at these low pressures hillocks formed on top of continuous films. The height of the hillocks decreases with increasing pressure.

The origin and formation mechanism of voids in the substrate during carbonization have not been fully explained in the past and deserve further study. Shown in Fig. 4a is a cross-sectional SEM microphotograph of one such void present in the Si substrate after an SiC film is grown at 760 Torr. The film over the void is uniform and continuous in this case. The void base and sides are about 1 μm in length. The SiC film surface morphology on the substrate (or "bottom") side is shown in Fig. 5a, where the Si substrate has been removed in an HNA ($HF:HNO_3$:acetic acid = 3:5:3) etching solution. The film bottom surface displays regions of grass-like growth located at void sites. These regions take a roughly square or triangular shape on (100) and (111) substrates, respectively. Thin leaf-like growth on the edge of each region is probably due to SiC growth on the void sidewalls. SiC films grown at low pressure exhibit significantly larger density of voids, and hence of grass-like growth, than films grown at atmospheric pressure. A cross-sectional SEM photo (Fig. 4b) of a film grown at low pressure (5 Torr) reveals the downward growth of the grass-like features into a void, and the formation of very thin layers on the void walls. For SiC growth at even lower pressure, 22 mTorr in the case of Fig. 4c, voids form even at locations into the Si substrate which are separated from the film/substrate interface by an Si region. The exact mechanism for this behavior is not clear at the present. However, a change in diffusion coefficient at this low pressure might be responsible.

While in most cases a completely continuous SiC film covers the voids, a careful investigation revealed that some voids are not completely sealed but have a small aperture in the film. Plan view and cross-sectional SEM microphotographs of an unsealed hole over a void in the substrate (dark square in plan view) are shown in Fig. 6a and b, respectively. An SEM microphotograph of a void which has just been sealed is shown in Fig. 6c for comparison. As discussed below, whether and when a void becomes sealed depends mainly on precursor concentration, growth pressure, and reaction time.

In the case of low pressure growth, we suspect that the center of each hillock is not sealed. Even though it is difficult to prove this directly, the cross-sectional SEM microphotograph shown in Fig. 7a appears to indicate that there exists an unsealed channel at the hillock center. A schematic corresponding to the microphotograph is shown in Fig. 7b. The existence of unsealed channels at the center of each hillock is vital to the explanation of continued film growth after a continuous SiC layer has been formed at low pressure.

To determine whether unsealed channels exist in each hillock of SiC films grown at 5 Torr we have anodically etched the SiC/Si substrates. Anodic etching is known to

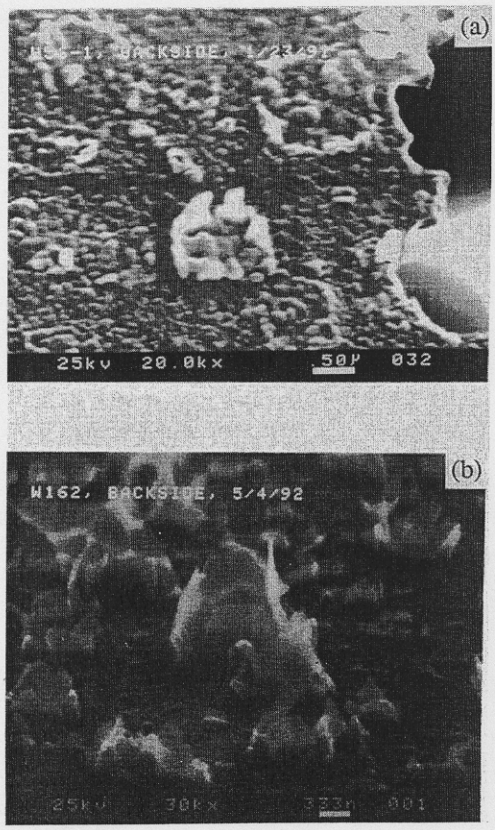

Fig. 5. SEM microphotographs of bottom surface of films grown on (100) Si at (a) 760 and (b) 5 Torr.

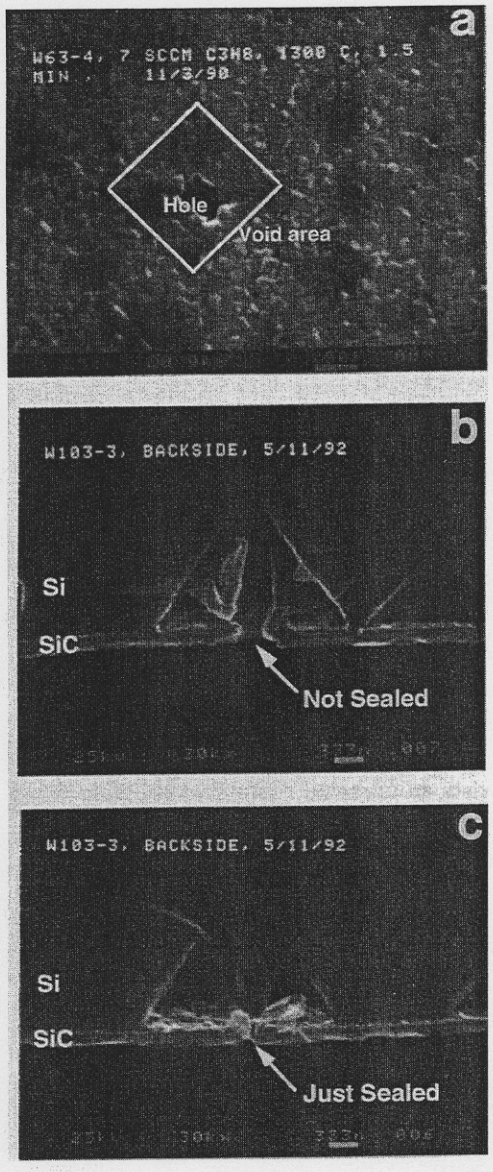

Fig. 6. Unsealed channels above voids in films grown at 760 Torr: (a) plan view SEM, (b) cross-sectional SEM, (c) a just-being-sealed void.

form a porous Si layer at the exposed Si surface.[24-29] The anodic etching for SiC films on Si was performed at a current density of 4 to 9 mA/cm^2 in a solution of 1:2:1 HF:ethanol:H_2O. The formation of a porous layer on void walls and at the void apex as shown in the SEM micrographs of Fig. 8a and b indicates that anodic etchant must enter the void, most likely by way of the unsealed channel at the hillock center in the film.

In order to study how SiC nuclei and Si voids are produced, growth was performed at a low precursor concentration to form individual SiC islands on the Si surface. Shown in Fig. 9a is a plan view SEM microphotograph of SiC islands formed on Si after growth at 1300°C for 90 s with low C_3H_8 partial pressure (4 sccm C_3H_8 and 0.9 slpm H_2). Each SiC island consists of dendritic features radiating from its center. Trenches are present in the Si substrate where islands are beginning to touch, as revealed by the corresponding cross-sectional SEM microphotograph in Fig. 9b. These trenches at the island boundaries are actually emerging voids in the Si substrate. Special attention should be paid to Fig. 9b because it exhibits a cross section obtained by cleavage through the center of two adjacent SiC islands. No voids or pits exist under the center of either island, whereas a void is observed being formed where the

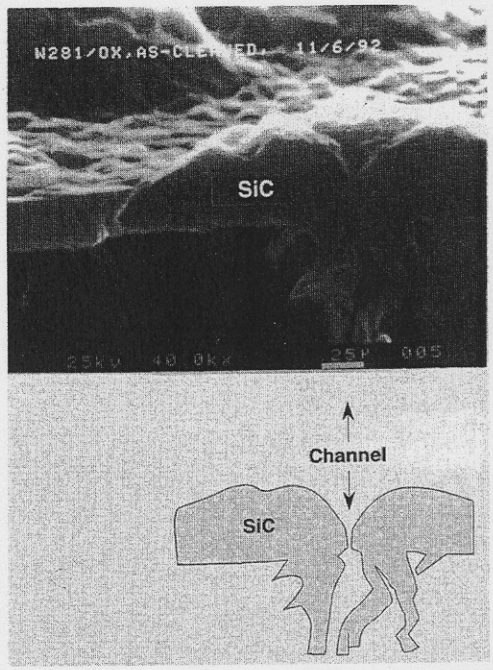

Fig. 7. Unsealed channel at the center of hillock in films grown at 5 Torr.

two islands are touching. This phenomenon of void formation along the boundaries between islands has been observed in all our carbonization experiments.

More quantitative information on the size and height of SiC islands was obtained by AFM. A typical AFM image of SiC islands on Si is shown in Fig. 10a. The gray scale z-axis (depth) is from 0 to 800 nm. It can be seen that the center of the island is at the highest point. The regions between islands are much darker, indicating the existence of deep

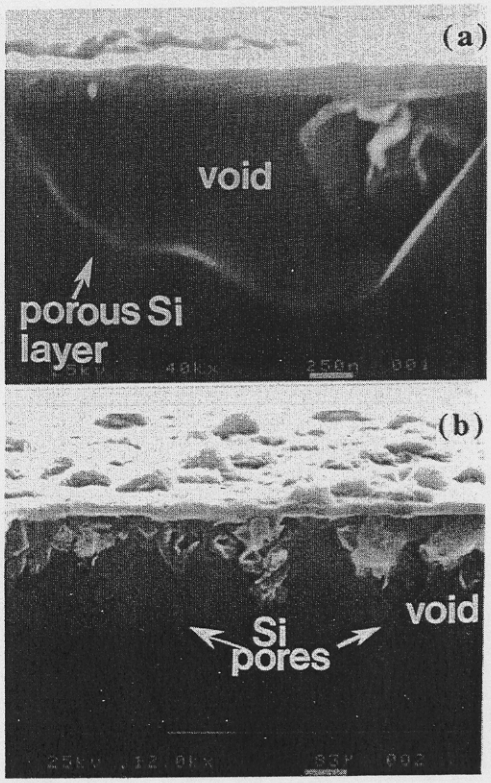

Fig. 8. Anodically etched SiC-on-Si to reveal unsealed channels in the film: (a) porous Si layer on void walls, (b) porous Si pores formed at apex of voids.

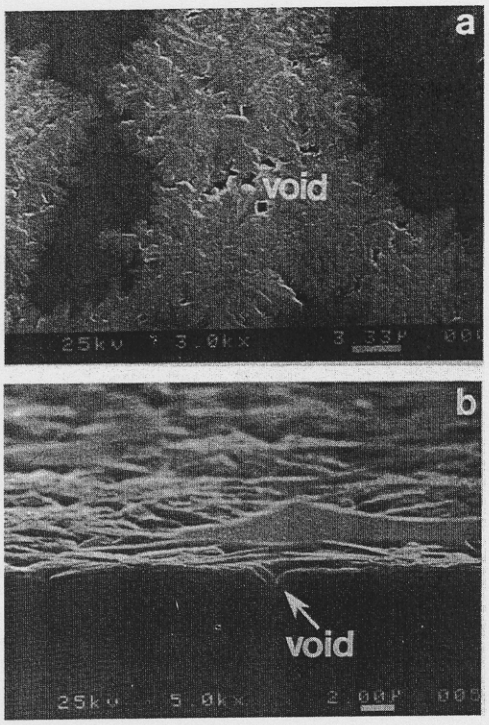

Fig. 9. Void formation along SiC island boundaries: (a) plan view SEM; (b) cross-sectional SEM.

trenches. A side view AFM image of a SiC film with a lower island density is shown in Fig. 10b. The flat region between islands is the unreacted Si surface. Trenches below the unreacted Si surface level are clearly observed around each SiC island. Line scans over the SiC islands have been used to quantitatively study the trenches around the islands.

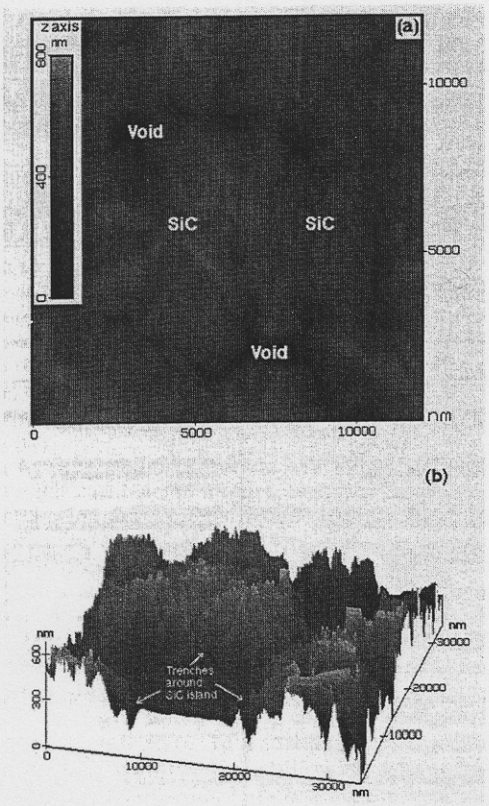

Fig. 10. AFM images of SiC islands: (a) top view, high density; (b) side view, lower density.

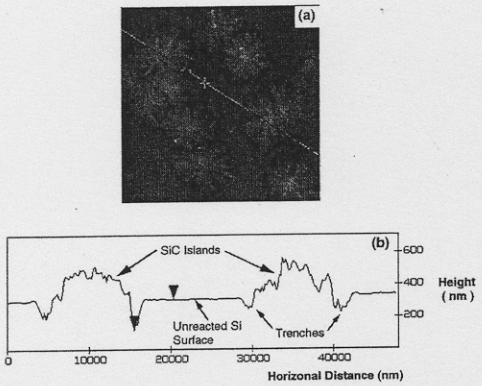

Fig. 11. Lower density SiC islands on Si: (a) AFM image, (b) AFM line scan along line indicated in (a).

One such scan is shown in Fig. 11. The indicated trench depth between the two arrow heads is 192 nm. In general, we have observed a range of trench depths from ~100 to ~200 nm. The height of the SiC islands above the Si surface is about 200 nm, which is comparable to the trench depth.

We have previously proposed[18] that the SiC nucleation density is determined primarily by the hydrocarbon partial pressure during growth. To confirm this nucleation model, a very short reaction time of nominally 1 s was used to perform carbonization with different C_3H_8 flow rates and a fixed (0.9 slpm) H_2 carrier gas flow rate. The growth was carried out at 1300°C with a temperature ramp-up rate of 50°C/s. Since the reaction time is extremely short, it is reasonable to assume that the reacted surface reflects the initial nucleation status. AFM analysis with the short-range scan head was then performed on each of the resulting

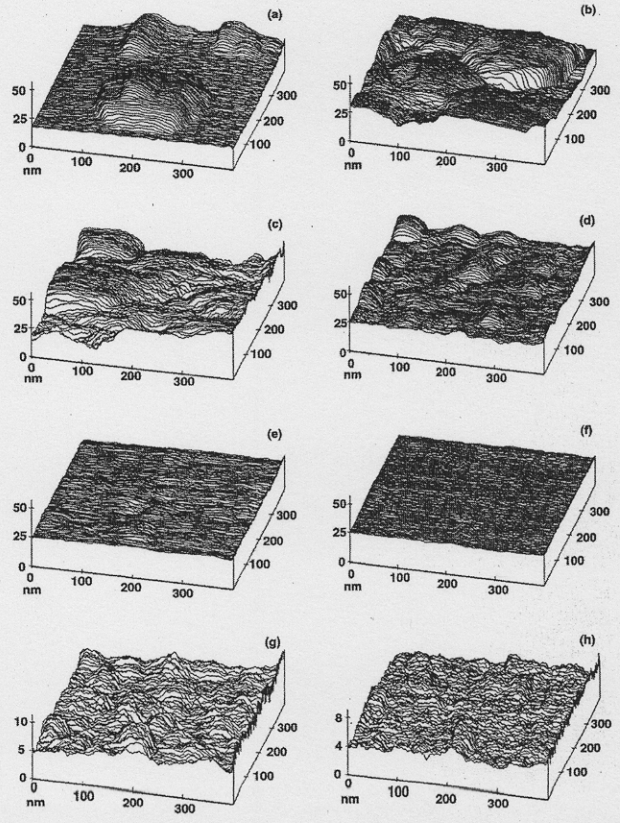

Fig. 12. AFM analysis of SiC films grown at 1300°C for 1 s *vs.* propane flow rates: (a) 2; (b) 4; (c) 7; (d) 9; (e) and (g) 12; (f) and (h) 20 sccm. Vertical scale is 0 to 50 nm for (a)-(f), 0 to 10 nm for (g), and 0 to 8 nm for (h).

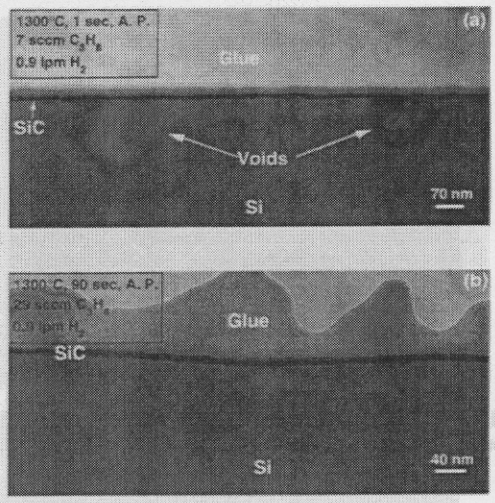

Fig. 13. Cross-sectional TEM of 10 nm films grown at (a) low propane flow for only 1 s, (b) high propane flow for 90 s.

films as shown in Fig. 12, where the flow rate is increasing from 2 sccm in Fig. 12a to 20 sccm in Fig. 12f. The gray scale in z-axis (depth) is from 0 to 50 nm for the images in Fig. 12a-f. AFM images with a smaller z range (8 to 10 nm) are shown in Fig. 12g and h for growth with 12 and 20 sccm, respectively. As can be seen, grain size and film roughness decrease with increasing propane flow rate. The film surfaces obtained at high flow rates are almost featureless. The grain density, and thus the nucleation density, is observed to increase with increasing propane flow rate.

The effect of nucleation on the formation of voids is clearly shown in Fig. 13. The film thickness of samples in Fig. 13a and b are both about 10 nm even though they are grown at 1300°C for 1 and 90 s, respectively. The corresponding flow conditions are 7 sccm (~transition concentration) and 30 sccm (>>transition concentration) C_3H_8 with 0.9 slpm H_2 carrier gas. Two voids in their early stage of formation are observed even after only 1 s in the film grown at the transition concentration (Fig. 13a). However, in the case of high concentration, no detectable voids are observed in the substrate even after a reaction time of 90 s.

The evolution of void formation with carbonization time at low pressure was studied. The surface conditions of films grown for times from 1 s to ~1 min are shown in Fig. 14. The surface morphology after 1 s at 1200°C, as shown in Fig. 14a, reveals a uniform distribution of fine SiC grains.

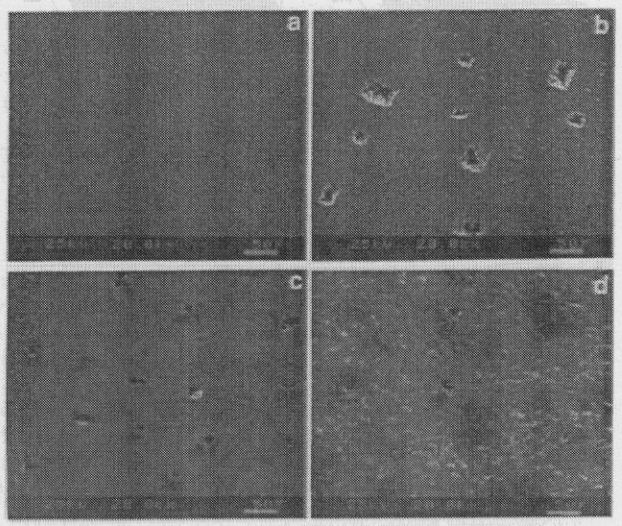

Fig. 14. Morphology of SiC films grown at 5 Torr as a function of growth time: (a) 1200°C, 1 s; (b) 1300°C, 1 s; (c) 1300°C, 15 s; (d) 1300°C, 45 s.

Table I. Comparison of experimental observations.

Mogab and Learny[4]	This work
A. Film thickness α P (for $P < P_t$).	A. Similar observation.
B. Thinner film at high P (for $P > P_t$).	B. Similar observation.
C. Voids in substrate; hillocks on film surface	C. Voids in substrate, unsealed holes in the film; hillocks on films grown at low pressures. 1. Nucleation density increases and nuclei size decreases with increasing P. 2. Trenches seen around individual SiC islands. 3. Voids at island boundaries, not at island center. 4. Film region over voids: not porous or polycrystalline.

P: hydrocarbon partial pressure.
P_t: transition hydrocarbon partial pressure.

However, after 1 s at 1300°C, Fig. 14b, voids begin to form while the grains grow larger in size. Continued carbonization at 1300°C for up to 15 s resulted in a smoother surface, Fig. 14c, which was thought to be due to the coherent agglomeration of fine grains. Openings in the film are observed along with film growth over voids. The surface after 45 s of the reaction is shown in Fig. 14d. Voids (dark features in the SEM micrograph) and unsealed holes over most voids are still observed. The surface morphology is rougher compared to the previous case shown in Fig. 14c.

Discussion

The experimental observations presented above contribute to support the argument that SiC thin film growth by carbonization of Si proceeds in the following sequence: (*i*) SiC nuclei formation, (*ii*) SiC nuclei growth and Si trench formation, (*iii*) the emergence of Si voids and the lateral extension of the SiC film over the void, and (*iv*) sealing of the void and formation of a continuous film over the void. In other words, in our model the void is formed prior to the growth of the film which covers it.

The AFM results obtained on SiC island density as a function of precursor flow rate (as shown in Fig. 12) are a direct evidence that the initial nucleation density is strongly determined by the precursor concentration during reaction.

This observation along with the growth rate and morphology characteristics in Fig. 1a, 2, and 3 can be explained based on the classical nucleation theory. To state it briefly,

Table II. Comparison of proposed mechanisms.

Mogab & Learny [4]	This Work
	0. Initial nucleation density α P.
1. SiC nuclei grow by consuming uniformly the unreacted Si.	1. SiC nuclei grow by consuming within a limited region unreacted Si.
2. Localized pitting --> porous material formation between nuclei.	2. Demand for Si and diminishing Si surface --> void formation in Si substrate.
3. Supply of Si for further growth comes from diffusion through porous defects.	3. Supply of Si for further growth comes through unsealed holes in the film.
	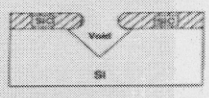
4. Porous defects sealed off at high P --> thinner film.	4. High nucleation density at high P --> quick nuclei coalescence and formation of a continuous, ultra-thin film.
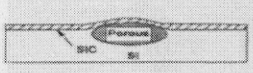	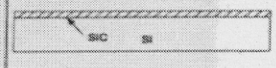
5. SiC nuclei: epitaxial at low P, random at high P.	5. Opposite finding.
	6. Voids location not at original nucleation site.

P - hydrocarbon partial pressure.

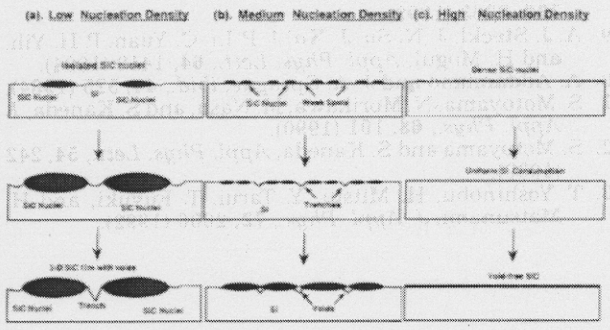

Fig. 15. Void formation and nucleation mechanism schematic diagram: (a) low, (b) medium, and (c) high nucleation density.

in a vapor-phase homoepitaxial growth on a single-crystal substrate, an over-saturated vapor condition created by lowering the substrate temperature leads to two-dimensional growth of thin and smooth films. On the other hand, an undersaturated condition will lead to thicker film through three-dimensional growth. In the case of SiC nucleation by carbonization, the minimum C_3H_8 concentration for continuous film formation can be thought to be the onset of the oversaturated C_3H_8 condition. Therefore, the highly oversaturated C_3H_8 gave rise to layer-by-layer growth of thin SiC films, while the undersaturated C_3H_8 condition resulted in cluster (island) formation of thicker SiC films.

These observations lead us to the following model for SiC growth on Si by carbonization: (*i*) the supply of Si for the vertical, as well as lateral growth, of SiC islands comes from the exposed, unreacted Si area around each island; (*ii*) the continuous demand for Si for the carbonization reaction, along with the fact that the available (unreacted) Si surface area is decreasing with increasing island diameter and density, drives the consumption of Si atoms in the vertical direction leading to formation of voids.

As in the case of much thinner film formation at high precursor concentration, voids have been observed during carbonization in the past by many other researchers[4,5,8,9] with various growth systems and growth conditions being used. For example, Learn and Khan,[5] Mogab and Leamy,[4] Khan and Summergrad[2] observed voids in their high vacuum carbonization system using C_2H_2. Addamiano,[30] Liaw and Davis,[9] Powell *et al.*[8] also observed voids with their atmospheric growth reactor using either C_2H_4 or C_3H_8. Recent gas source molecular beam epitaxy (GSMBE) studies of SiC growth on Si by Motoyama *et al.*[31,32] and Yoshinobu *et al.*[33] reported hillock formation on the film surface in addition to voids in the Si substrate.

Previously, the mechanisms of SiC nucleation and void formation were incorporated in a model proposed by Mogab and Leamy.[4] The M-L model explained many of the features of Si carbonization and was widely adopted. For example, this model has been used by Yoshinobu *et al.*[33] to select growth conditions which suppress pits and hillock formation.

In this work, we have presented new experimental information which can lead to a more complete understanding of the nucleation and void formation mechanisms. A comparison of experimental observations and proposed models of SiC nucleation mechanism between M-L and the present authors is shown in Tables I and II. The comparison of experimental observations (Table I) indicates that similar results were obtained with regard to film thickness dependence on hydrocarbon partial pressure (P), for values both larger and smaller than the transition partial pressure (P_t). At the heart of both models is the common observation of voids in the Si substrate. In addition, our experimental observations have confirmed the following salient features of the carbonization process: 1, increasing the hydrocarbon partial pressure leads to a decrease in nuclei size and an increase in their density; 2, trenches in the Si substrate surround individual SiC islands during carbonization; 3, voids occur at trench locations coincident with SiC inter-island boundaries during film growth; 4, the SiC film overlying the void is crystalline, not porous or polycrystalline. Our model regarding nucleation mechanism agrees with the M-L model only in that SiC nuclei grow by consuming unreacted Si. The major differences between our model and the M-L model are: 1, voids, rather than porous material, are formed at nuclei boundaries when they grow together; 2, thinner films and cessation of growth after a certain reaction time at high hydrocarbon partial pressure are due to the negligible Si diffusion through a thin, but continuous, SiC layer rather than to the sealing-off of porous defects in the film. This layer is formed quickly by the coalescence of the high initial density SiC nuclei. Schematic diagrams depicting our model are shown in Fig. 15 for cases of low, medium, and high nucleation density.

Summary

Based on SEM and AFM analyses of SiC films grown on Si by RTCVD, a model for void formation and SiC nucleation has been proposed, consisting of the following main points: (*i*) the initial nucleation density is determined by the precursor concentration in the reaction gas; (*ii*) each nucleus grows larger both laterally and vertically by consuming the Si around it; (*iii*) voids are not located at the original nucleation sites, but rather are formed when nuclei grow to the point of contact.

Acknowledgments

The authors appreciate the support of this work by the NASA Space Engineering Research Center at the University of Cincinnati. The assistance of M. W. Roth and S. Mogren with the AFM study is also acknowledged. Finally, many very useful discussions on SiC growth with J. A. Powell, L. G. Matus (an early proponent of using RTCVD to study SiC nucleation), and P. Pirouz are greatly appreciated.

Manuscript submitted May 27, 1994; revised manuscript received Sept. 19, 1994.

REFERENCES

1. J. Graul and E. Wagner, *Appl. Phys. Lett.*, **21,** 67 (1972).
2. I. H. Khan and R. N. Summergrad, *ibid.*, **11,** 12 (1967).
3. H. Nakashima, T. Sugano, and H. Yanai, *Jpn. J. Appl. Phys.*, **5,** 874 (1966).
4. C. J. Mogab and H. J. Leamy, *J. Appl. Phys.*, **45,** 1075 (1974).
5. A. J. Learn and I. H. Khan, *Thin Solid Films*, **5,** 145 (1970).
6. S. Nishino, J. A. Powell, and H. A. Will, *Appl. Phys. Lett.*, **42,** 460 (1983).
7. K. Sasaki, E. Sakuma, S. Misana, S. Yoshida, and S. Gonda, *ibid.*, **45,** 72 (1984).
8. J. A. Powell, L. G. Matus, and M. Kuczmarski, *This Journal*, **134,** 1559 (1987).
9. P. Liaw and R. F. Davis, *ibid.*, **132,** 642 (1985).
10. H. S. Kong, T. C. Wang, J. T. Glass, and R. F. Davis, *J. Mater. Res.*, **3,** 521 (1988).
11. A. Suzuki, K. Furukawa, Y. Higashigaki, S. Harada, S. Nakajima, and T. Inoguchi, *J. Cryst. Growth*, **70,** 287 (1984).
12. H. J. Kim and R. F. Davis, *This Journal*, **134,** 2269 (1987).
13. S. R. Nutt, D. J. Smith, H. J. Kim, and R. F. Davis, *Appl. Phys. Lett.*, **50,** 203 (1987).
14. P. Pirouz, F. Ernst, and T. T. Cheng, *MRS Symp. Proc.*, **116,** 57 (1988).
15. F. Ernst and P. Pirouz, *J. Mater. Res.*, **4,** 834 (1989).
16. M. Iwami, M. Hirai, M. Kusaka, Y. Yokota, and H. Matsunami, *Jpn. J. Appl. Phys.*, **28,** L293 (1989).
17. J. P. Li, A. J. Steckl, I. Golecki, F. Reidinger, L. Wang, X. J. Ning, and P. Pirouz, *Appl. Phys. Lett.*, **62,** 3135 (1993).
18. A. J. Steckl and J. P. Li, *IEEE Trans. Electron Devices*, **ED-39,** 64 (1992).
19. A. J. Steckl and J. P. Li, *MRS Symp. Proc.*, **242,** 537 (1992).
20. A. J. Steckl and J. P. Li, *Thin Solid Films*, **216,** 149 (1992).
21. G. Meyer and N. M. Amer, *Appl. Phys. Lett.*, **53,** 1045 (1988).

22. P. K. Hansma, V. B. Elings, O. Marti, and C. E. Bracken, *Science*, **242**, 209 (1988).
23. S. Dror, *Scanning Force Microscopy*, Oxford University Press, New York (1991).
24. A. Uhlir, *Bell Sys. Tech. J.*, **35**, 333 (1956).
25. A. Gee, *This Journal*, **107**, 788 (1960).
26. R. Memming and G. Schwandt, *Surf. Sci.*, **4**, 109 (1966).
27. M. A. Tischler, R. T. Collins, J. H. Stathis, and J. C. Tsang, *Appl. Phys. Lett.*, **60**, 639 (1992).
28. K. H. Jung, S. Shih, and D. L. Kwong, *This Journal*, **139**, 3363 (1992).
29. A. J. Steckl, J. N. Su, J. Xu, J. P. Li, C. Yuan, P. H. Yih, and H. Mogul, *Appl. Phys. Lett.*, **64**, 1419 (1994).
30. A. Addamiano and J. A. Sprague, *ibid.*, **44**, 525 (1984).
31. S. Motoyama, N. Morikawa, M. Nasu, and S. Kaneda, *J. Appl. Phys.*, **68**, 101 (1990).
32. S. Motoyama and S. Kaneda, *Appl. Phys. Lett.*, **54**, 242 (1989).
33. T. Yoshinobu, H. Mitsui, Y. Tarui, T. Fuyuki, and H. Matsunami, *J. Appl. Phys.*, **72**, 2006 (1992).

Reprinted from JOURNAL OF THE ELECTROCHEMICAL SOCIETY
Vol. 142, No. 2, February 1995
Printed in U.S.A.